Chaos Analysis of Transcranial Doppler Signals for Feature Extraction

Ali Ozturk
Computer Engineering Department, KTO Karatay University, Konya, Turkey
Havelsan Inc., Ankara, Turkey

Keywords: Chaos Analysis, TCD Signals, Correlation Dimension, Maximum Lyapunov Exponent, Recurrence Plots, Chaotic Attractors, Space-Time Separation Plots.

Abstract: In this study, chaos theory tools were used for feature extraction from Transcranial Doppler (TCD) signals. The surrogates data sets of the TCD signals which were used for the nonlinearity analysis were extracted as the first feature set. The nonlinear cross prediction errors which were used for the stationary analysis were also extracted for the TCD signals as another feature set. The chaotic invariant features like correlation dimension, maximum Lyapunov exponent, recurrence quantification measures etc. give quantitative values of complexity of the TCD signals. The correlation dimension and maximum Lyapunov exponent were already used as features for classification of TCD signals in the literature. As another chaotic feature set, the statistical quantitative values were extracted from the recurrence plots. The correct calculation of the time delay and the minimum embedding dimension is crucial to correctly estimate all of the chaotic features. These two data were calculated via mutual information and false nearest neighbours approaches, respectively. The space-time separation plots were used in order to find the ideal dimension of Theiler window *w* which is another important value for the correct estimate of chaotic measures. The reconstructed chaotic attractors with 3-D embedding and 1-step time delay represent the visual phase space portrait of the TCD signals. The attractors were also suggested as another candidate feature set.

1 INTRODUCTION

TCD study of the adult intracerebral circulation is used to evaluate intracranial stenoses, cerebral arteriovenous malformations, cerebral vasospasm and cerebral hemodynamics in general (Evans et al.., 1989). The blood flow anomalies in the cerebral vessels can be visually observed in the sonograms. However, properly enabling the expert medical staff to interpret TCD signals is difficult and this prevents their wider and effective usage in the clinics.

In the literature, the linear features extracted from Doppler signals via spectral analysis methods were used for automatic medical diagnosis (Ubeyli and Guler, 2005; Guler et al., 2002). The spectral features of TCD signals were used for the performance comparison of two different artificial neural networks in (Serhatlioglu et al., 2003) for the classification of the TCD signals.

There are various studies in which chaos theory methods were used to analyse the Doppler signals (Keunen et al., 1994; Vliegen et al., 1996). Keunen et al., (1996) suggested that the TCD signals of healthy subjects have an underlying nonlinear dynamics. It was recognized by Visee et al., (1995) that the nonlinear phenomena were lost in ischemic cerebrovascular territory in patients with occlusive cerebrovascular disease while there was nonlinearity detected in noncompromised side.

Two chaotic invariant measures, i.e. the correlation dimension and maximum Lyapunov exponent, were used for the classification of TCD signals in (Ozturk and Arslan, 2007; Ozturk et al., 2008) to compare the performance of various classifiers. The performance of the chaotic and linear features were compared on a neuro-fuzzy classifier in (Ozturk and Arslan, 2015).

If linear methods are used to analyse a time series which is generated by a nonlinear process, then some critical features of it can remain undetected and most of it can be considered as noise. The non-linear time series analysis (chaos theory) provided some tools to quantitatively analyse a time series which is generated by an underlying nonlinear process. However, in order to apply nonlinear time

Ozturk, A.
Chaos Analysis of Transcranial Doppler Signals for Feature Extraction.
DOI: 10.5220/0005693701680174
In *Proceedings of the 9th International Joint Conference on Biomedical Engineering Systems and Technologies (BIOSTEC 2016) - Volume 4: BIOSIGNALS*, pages 168-174
ISBN: 978-989-758-170-0

series analysis (chaos theory) methods, it must be proven that the signals are both nonlinear and stationary. In (Ozturk and Arslan, 2007), the surrogates data method was used to detect the nonlinearity of TCD signals. In this study, The surrogates data set of the TCD signals were extracted as the first feature set. The stationarity of the TCD signals is detected with nonlinear cross prediction errors method in (Ozturk and Arslan, 2007). In this study, this method was used to extract the non-linear cross prediction values as another feature set.

The most famious chaotic features used in the literature are the maximum Lyapunov exponent and the correlation dimension. These chaotic measure will eventually be different for a specific time series generated by a specific natural phenomea, since each chaotic attractor will have a different picture in the embedded phase space. These two features were also mentioned as a different feature set in this study.

The recurrence plots are mainly used for nonstationarity analysis and visualization of time series. The visual data in the recurrence plots is hard to interpret. Therefore, recurrence quantification analysis is necessary to quantify the number and duration of recurrences which is presented by the state space trajectory of a dynamical system. The other proposed feature set in this study is the statistical quantitative values which are extracted from the recurrence plots of TCD signals. The time delay information and minimum embedding dimension play important role for the correct extraction of all chaotic features. This is also true for recurrence quantification analysis. The other important parameter which effects all of the results is the Theiler window *w* and it is estimated from the space-time separation plots.

The reconstructed 3-D chaotic attractors of the TCD signals were also presented. These can be used to extract a different set of features via image processing methods.

2 MATERIALS AND METHOD

2.1 Hardware

The hardware of the system used for this study involves a 2 Mhz ultrasound transducer, analog Doppler unit (Multi Doppler Transducer XX, DWL Gmb, Uberlingen, Germany), analog/digital interface board (Sound Blaster Pro-16), and PIII 600 Mhz microprocessor PC with printer. The Doppler unit is also equipped with imaging software that makes it possible to focus the sample volume at a desired location in the temporal region. The signal obtained from the blood vessel is transferred to a PC via a 16-bit sound card on an analog/digital interface board (Ozturk et al., 2008). The signals were then sampled to 0-255 interval as shown in Figure 1.

2.2 Surrogates Data Set

The method of Iterative Amplitude Adjusted Fourier Transform (IAAFT) discussed in (Schreiber and Schmitz, 1996) is used to generate surrogate data sets. The Fourier-based surrogates depend on the idea of creating constrained realizations. In this approach, the measurable properties of the time series are taken into account. The linear properties of the time series are specified as in the following

$$\left|S_k\right|^2 = \left|\frac{1}{\sqrt{N}}\sum_{n=0}^{N-1} s_n e^{i2\pi kn/N}\right|^2 \quad (1)$$

The surrogate time series are created by multiplying the Fourier transform of the data by random phases and then transforming back to the time domain as:

$$\bar{s}_n = \frac{1}{\sqrt{N}}\sum_{k=0}^{N-1} e^{i\alpha_k}\left|S_k\right| \; e^{-i2\pi kn/N} \quad (2)$$

Where $0 \le \alpha_k < 2\pi$ are independent uniform random numbers.

2.3 Nonlinear Cross Prediction Errors Data Set

The method used for the stationarity test of the TCD signals in (Ozturk and Arslan, 2007) was utilized to extract the non-linear cross prediction errors as another feature set. This method divides the time series into equal parts and the simple nonlinear prediction algorithm (Hegger et al., 1999) is applied to the segments to find the one-step ahead prediction errors. The embedding vectors were obtained by embedding the time series in 3-D phase space with a time delay of 1. In the delay embedding space, all neighbours of s_n are taken into account in order to make a prediction at time $n + k$.

$$s_{n+\Delta k} = \frac{1}{|\mathcal{U}_\epsilon(s_n)|}\sum_{s_n \in \mathcal{U}_\epsilon(s_n)} s_{n+\Delta k} \quad (3)$$

Where $|\mathcal{U}_\epsilon(s_n)|$ is the number of elements in the neighbourhood $\mathcal{U}_\epsilon(s_n)$ of radius[3] ϵ around the point s_n.

The time series was divided into segments S_i, i=1,..,N. For each two segments S_i and S_j, the root

mean squared error was computed using the neighbours of S_i to predict S_j. For i=j, the cross prediction errors will be smallest, since S_i and S_j are identical.

For random time series such as white noise, the nonlinear cross prediction errors are close to 1. On the other hand, for a periodic signal which is generated by sinus function, they are close to 0. For the time series those are generated by natural processes, they generally lie in between.

2.4 Recurrence Plots

The other two common methods in nonstationarity analysis and visualization of time series are the recurrence plots (Eckmann et al., 1987) (Casdagli, 1997) and the time-seperation plots (Provenzale et al., 1997). It is difficult to interpret the recurrence plots due to their complexity (Webber and Zbilut, 1994). The points obtained from a time series belonging to a stationary process are spreaded over the plot homogenously, while the points of a time series belonging to non-stationary process are grouped around the diagonal (Sprott, 2002). If there are too many separated points in the plot, this indicates randomness. This occurs when there is too much noise in the time series or the embedding dimension is insufficient. If the points over the surface have no pattern then the process which generates the time series has no or very poor determinism (Kantz and Schreiber, 2005). Zbilut et.al (1998), extracted some statistical quantitative values from the recurrence plots. Some of these values are the surface coverage rate of the points (REC), the rate of the points parallel to the diagonal (DET), the length distribution of the points which form a straight line (ENT) indicating the rate of the deterministic structures in the time series and the regression coefficient (TREND) which represents the relationship between the distance from the diagonal and the recurrence number. The calculation of these values takes too long for huge time series. However, it was observed that for sub-sections of TCD time series, these values do not differ significantly and reflect the characteristics of the original time series.

$$REC = \frac{1}{N}\sum_{i,j=1}^{N} R_{i,j} \quad (4)$$

Where N is the total number of points in a recurrence plot and $R_{i,j} \in \{0,1\}$ depending of the existence of a point on the i-j coordinates.

$$DET = \frac{\sum_{l=l_{min}}^{N} lP(l)}{\sum_{i,j=1}^{N} R_{i,j}} \quad (5)$$

Where $P(l)$ is the histogram of the length l of the diagonal lines.

$$ENT = -\sum_{l=l_{min}}^{N} p(l)\ln p(l) \quad (6)$$

Where $p(l)$ corresponds to the diagonal line length.

$$TREND = \frac{\sum_{i=1}^{\tilde{N}} (i-\tilde{N}/2)(RR_i - \langle RR_i \rangle)}{\sum_{i=1}^{\tilde{N}} (i-\tilde{N}/2)^2} \quad (7)$$

Where $\tilde{N}$ is the maximal number of diagonals parallel to the main diagonal line. $\langle RR_i \rangle$ indicates the average of the recurrence points RR_i.

The values of the time delay, the minimum embedding dimension and the Theiler window are important for the calculation of the statistical quantitative measures mentioned above.

2.5 Space-time Separation Plots

In recurrence plots, the graph of the points which are closer than a specific ε distance value are obtained with absolute time. The space-time separation plots are obtained with relative time. In this kind of plots, if a vector on the reconstructed attractor has at least one neighbour in a specific δt interval and Δd distance, then it is marked as δt – Δd point. By means of these plots, it is possible to identify the temporary correlations and to find the dimension of the Theiler window w which is used in correlation dimension algorithm of Theiler (1990) and in Lyapunov exponent estimation of Kantz algorithm (Kantz, 1994). The first peak point which is close to the general height in the space-time separation point generally gives the ideal dimension of Theiler window w.

2.6 Correlation Dimension

The correlation dimension is computed most efficiently by the correlation sum (Grassberger and Procaccia, 1983):

$$C(m,\varepsilon) = \frac{1}{N_{pairs}} \sum_{j=m}^{N} \sum_{k<j-w}^{N} \Theta(\varepsilon - |s_j - s_k|) \quad (8)$$

Where s_i are m-dimensional delay vectors, $N_{pairs}=(N-m+1)(N-m-w+1)/2$ is the number of pairs of points covered by the sums, Θ is the Heaviside step function and w is the Theiler window (Theiler, 1990). The following power law exists between embedding dimension m, ball radius ε and correlation dimension D_2

$$C(m,\varepsilon) \propto \varepsilon^{D_2} \quad (9)$$

The correlation dimension D_2 can be defined as

$$D = \lim_{\epsilon \to 0} \lim_{N \to \infty} d(N,\epsilon) \quad (10)$$

Where

$$d(N,\epsilon) = \frac{\partial lnC(\epsilon,N)}{\partial ln\epsilon} \quad (11)$$

The minimum embedding dimension and the time delay between embedding vectors are crucial in order to estimate the correlation dimension correctly. For the calculation the time delay, the mutual information method suggested by Fraser and Swinney (1986) was used. In this method, the mutual information S is computed for different τ delay values,

$$S = -\sum_{ij} p_{ij}(\tau) \ln \frac{p_{ij}(\tau)}{p_i p_j} \quad (12)$$

Where p_i is the probability to find a time series value in the i-th interval, and $p_{ij}(\tau)$ is the joint probability that an observation falls into the *i*-th interval and the observation time τ later falls into the *j*-th interval. The time delay τ where the mutual information S takes the first minimum value is the optimum delay and is used for embedding.

We used the false nearest neighbors method proposed in (Hegger et al., 1999) to find the minimum embedding dimension. This method includes some small changes to the original algorithm proposed by (Kennel et al., 1992) to avoid the wrong results due to the noise in the time series. Assuming that the standard deviation of the time series is σ, the threshold of false nearest neighbors is r and the distance between the vectors of the phase space is found according to maximum difference, the false nearest neighbors statistics is calculated as in the following:

$$X_{SYK}(r) = \frac{\sum_{n=1}^{N-m-1} \Theta\left(\frac{\left|S_n^{(m+1)} - S_{k(n)}^{(m+1)}\right|}{\left|S_n^{(m)} - S_{k(n)}^{(m)}\right|} - r\right) \Theta\left(\frac{\sigma}{r} - \left|S_n^{(m)} - S_{k(n)}^{(m)}\right|\right)}{\sum_{n=1}^{N-m-1} \Theta\left(\frac{\sigma}{r} - \left|S_n^{(m)} - S_{k(n)}^{(m)}\right|\right)} \quad (13)$$

Where, $S_{k(n)}^{(m)}$ is the nearest neighbour of the vector S_n and k(n) is the index of the time series which is different than n and supplying the condition of $|S_n - S_k|$ being minimum. The second Heaviside function in the nominator is used to eliminate the vectors of which initial distances are higher than σ/*r*. The same function also exists in the denominator for the same reason.

2.7 The Maximal Lyapunov Exponent

In the phase space, the distances between embedding vectors on attractor do not grow everywhere with the same rate. They may shrink locally. Therefore, the maximal Lyapunov exponent calculation will be the average of the local divergence rates over the whole embedding vectors.

The algorithm developed by Rosenstein et. al. (1993) was used to find the maximal Lyapunov exponent. This algorithm computes the local divergence rates of the state space distances over the whole time series data. The stretching factor S is found for different N values as in following

$$S = \frac{1}{N}\sum_{n_0=1}^{N} \ln\left(\frac{1}{\left|\vartheta_{Xn_0}\right|}\sum\left|X_{n_o} - X_n\right|\right) \quad (14)$$

Where, X_{n_0} is an embedding vector on the attractor, X_n are the neighboring vectors within diameter ϵ and ϑ_{Xn_0} is the number of these neighbors.

The first slope of the curve obtained by plotting S values for various N values on x-y coordinate system gives the maximal Lyapunov exponent.

3 EXPERIMENTAL RESULTS AND DISCUSSION

The profile of the subjects from which the TCD signals were obtained is given in the following table.

Table 1. The profile of the subjects used in this study.

	Males	Females	Age Range	Avg. Age
Cerebral aneurysm	12	8	55-65	59.5±0.5
Brain Hemorrhage	4	6	21-36	27.0±0.5
Cerebral Oedema	11	11	3-40	25.0±0.5
Brain Tumor	12	18	12-41	29.5±0.5
Healthy	15	8	23-65	31.5±0.5
Summary	54	51	3-65	35.0±0.5

The Iterative Amplitude Adjusted Fourier Transform (IAAFT) method is used to generate the surrogate data sets for each TCD signal. A sample surrogate data set for the TCD signal of a patient with cerebral aneurysm (Figure 1) is given in Figure 2. It is not easy to visually distinguish the surrogate data sets from the original TCD signal, but the surrogates are created with the linear properties via Fourier transform.

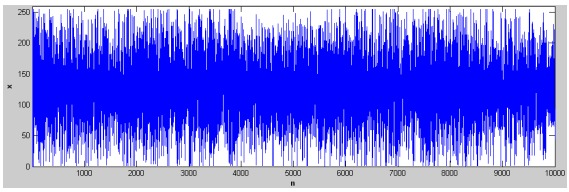

Figure 1: The TCD signal of a patient with cerebral aneurysm.

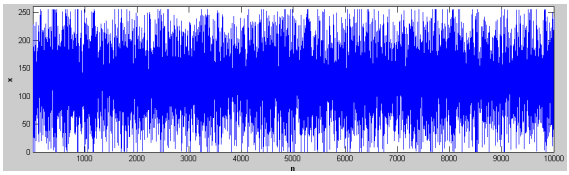

Figure 2: The surrogate time series generated for the TCD signal given in Figure 1.

In the following figure, it can be seen that the nonlinear cross-prediction error values for the TCD signals lie between pure deterministic (sinus signal) and random (Gaussian) time series. These values can be used as another feature set for the classification of the TCD signals.

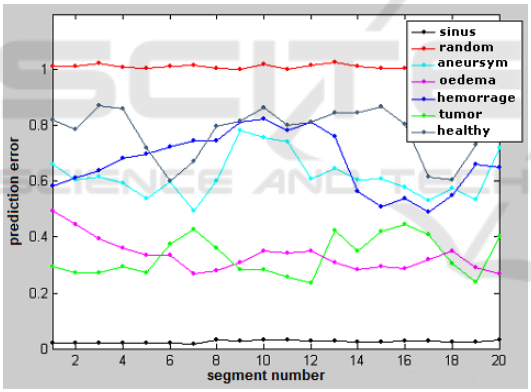

Figure 3: The non-linear prediction errors for sinus, Gaussian random and one for each TCD signals time series.

In the following figure, the recurrence-plots of the TCD signals belonging to different patient groups are given. As can be seen from the figures, each patient has a different structure within its recurrence-plot. The statistical quantitative values like REC, DET, ENT and TREND were calculated using the recurrence-plots of the TCD signals. These values constitute the other chaotic feature set

In the following figure, the space-time separation plots of the TCD signals belonging to different patient groups are given. In these plots, the first peak point which is close to the

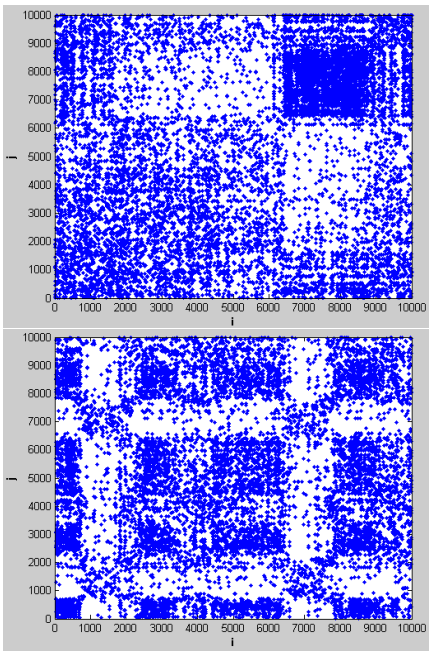

Figure 4: Recurrence plots of the TCD signals belonging to a patient of (a) Hemorrhage and (b) Healthy subject.

general height in the space-time separation point was used to identify the ideal dimension of Theiler window w.

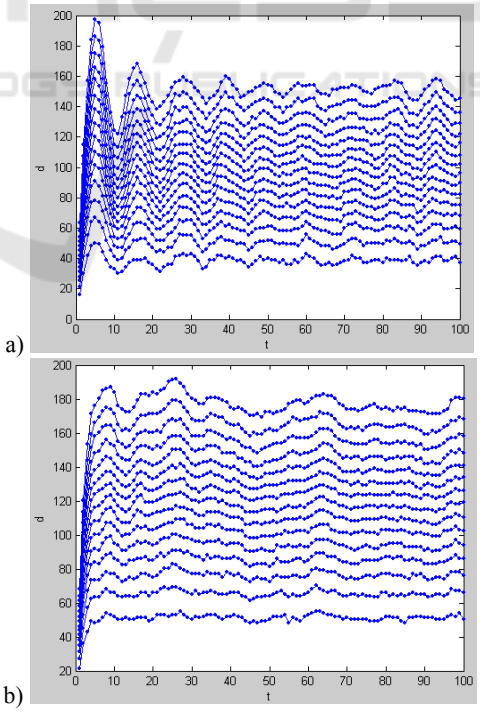

Figure 5: The space-time separation plot of the TCD signal with patient groups a) Oedema (w=50) b) Tumor (w=40).

The chaotic attractors embedded in 3-dimensions for each patient group are given in the following figure. The first 300 points of TCD signals were used to draw the attractors in order to enhance the visuality. The time delay used to draw the attractors was 1. These chaotic attractor pictures can be used to extract another feature set for the TCD signals.

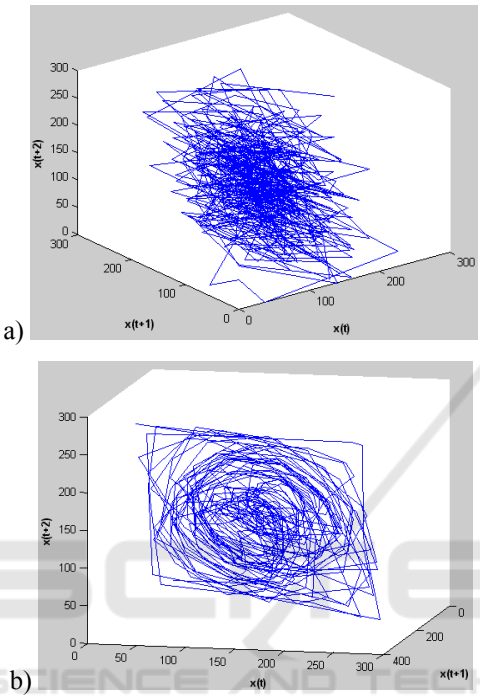

Figure 6: The chaotic attractors of the TCD signals embedded in 3-dimensions with 1 time delay a) Healthy b) Oedema.

In the following figure, the correlation dimension estimation for the TCD time series of a patient with brain hemorrhage is given as an example.

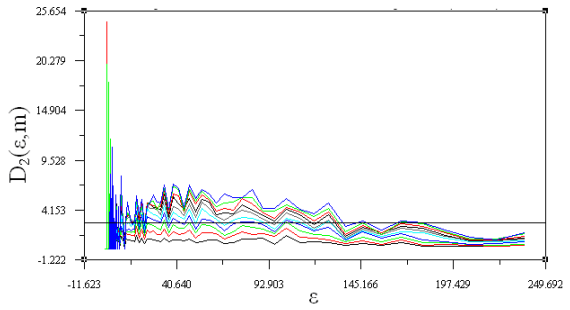

Figure 7: Correlation dimension estimation of a patient with brain hemorrhage.

For all of the chaotic features, we need time delay information which is obtained by mutual information method. According to this method, the first delay value τ at which time delayed mutual information takes the minimum is a good candidate for a reasonable time delay. In the following figure, the time delay estimation for the TCD signals with brain oedema is given.

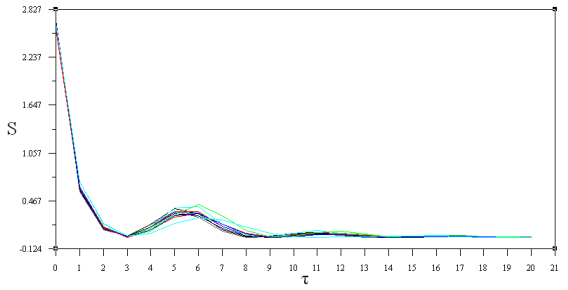

Figure 8. Time delay value estimation for the patients with brain oedema.

In the following figure, it is shown how the maximal Lyapunov is calculated for a patient with cerebral aneurism.

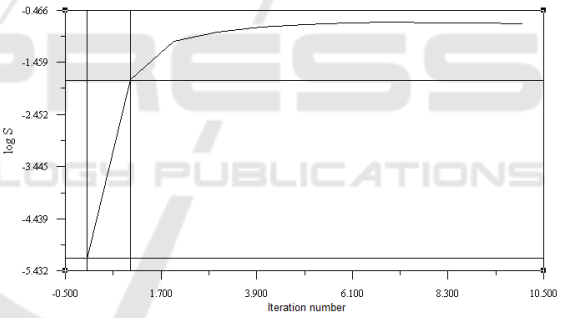

Figure 9: Maximal Lyapunov exponent estimation for the TCD signal of a patient with cerebral aneurism.

In the following figure, the minimum embedding dimension estimation for the TCD signals with brain tumor is given.

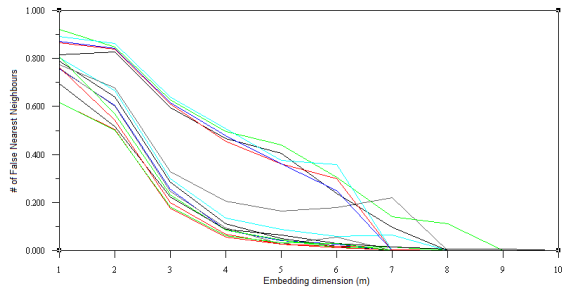

Figure 10: Minimum embedding dimension estimation for some of the patients with brain tumor.

4 CONCLUSIONS

Besides the chaotic invariant measures such as correlation dimension and maximal Lyapunov exponent, some other feature sets which can be extracted with non-linear time series analysis may be used to further evaluate some of the brain vessel diseases. The chaotic invariant measures may be supported with these feature sets. These features alone or with chaotic measures together may be used to train a classifier. After the generalization, the classifier may be used to make automatic diagnosis of the brain diseases.

The non-linear cross prediction errors of the TCD signals and the statistical quantitative values extracted from the recurrence plots can also be used to train various classifiers in order to make automated diagnosis of the brain vessel diseases.

The reconstructed 3-D chaotic attractor pictures can be used to extract another feature set for the TCD signals.

REFERENCES

Casdagli, M., 1997. *Recurrence plots revisited*. Physica D. 108:12-44.

Eckmann, J.P., Oliffson, K.S., Ruelle, D., 1987. *Recurrence plots of dynamical systems*. Europhys. Lett. 4(9): 973-977.

Evans, D.H., McDicken, W.N., Skidmore R., Woodcock, J.P., 1989. *Doppler Ultrasound: Physics, Instrumentation and Clinical Applications*. Wiley, Chichester.

Fraser, A. M., Swinney, H. L. 1986. *Independent coordinates for strange attractors from mutual information*, Phys. Rev. A 33: 1134.

Guler, I., Hardalac, F., Barisci N., 2002. *Application of FFT analyzed cardiac Doppler signals to fuzzy algorithm*, Comp. Biol. Med. 32:435–444.

Grassberger, P., Procaccia, I., 1983. *Characterization of Strange Attractors*. Physical Review Letters, 50:346-349.

Hegger, R., Kantz, H., Schreiber, T., 1999. *Practical implementation of nonlinear time series methods*: *The TISEAN package*. Chaos, 9: 413.

Kennel, M. B. Brown, R., Abarbanel, H. D. I., 1992. *Determining embedding dimension for phase-space reconstruction using a geometrical construction*. Physics Rev. A. 45: 340-353.

Keunen, R.W., Pijlman, H.C., Visee, H.F., Vliegen, J.H., Tavy, D.L., Stam, K.J., 1994. *Dynamical chaos determines the variability of transcranial Doppler signals*, Neurol. Res. 16: 353–358.

Keunen, R.W., Vliegen, J.H., Stam, C.J., Tavy, D.L., 1996. *Nonlinear transcranial Doppler analysis demonstrates age-related changes of cerebral hemodynamics*, Ultrasound Med. Biol. 22:383–390.

Kantz, H., 1994. *A robust method to estimate the maximal Lyapunov exponent of a time series*. Phys. Lett. A. 185: 77-87.

Kantz, H., Schreiber T., 2005. *Nonlinear Time Series Analysis*, Cambridge University Press.

Ozturk, A., Arslan A., 2007. *Classification of transcranial Doppler signals using their chaotic invariant measures*, Computer Methods and Programs in Biomedicine, 86(2): 171-180.

Ozturk A., Arslan A., Hardalac F., 2008. *Comparison of neuro-fuzzy systems for classification of transcranial Doppler signals with their chaotic invariant measures*, Expert Systems with Applications, 34(2): 1044-1055.

Ozturk A., Arslan A., 2015. *Neuro-fuzzy Classification of Transcranial Doppler Signals with Chaotic Meaures and Spectral Parameters*, 3rd Science and Information Conference, 591-596.

Provenzale, A., Smith, L. A., Vio, R., Murante, G., 1992. *Distinguishing between low-dimensional dynamics and randomness in measured time series*, Physica D 58, 31.

Schreiber, T., Schmitz, A. 1996. *Improved surrogate data for nonlinearity tests*, Phys. Rev. Lett. 77, 635.

Schreiber, T., 1997. *Detecting and analysing non-stationarity in a time series with nonlinear cross-predictions*, Phys. Rev. Lett. 78:843.

Serhatlioglu S., Hardalac F., Guler I., 2003. *Classification of transcranial Doppler signals using artificial neural network*, J. Med. Syst. 27:205–214.

Sprott, J.C., 2002. *Chaos and Time-Series Analysis*, Oxford University Pres, New York.

Rosenstein, M. T., Collins, J. J., De Luca, C. J., 1993. *A practical method for calculating largest Lyapunov exponents from small data sets*, Physica D 65,: 117.

Theiler, J., 1990. *Estimating fractal dimension*. J. Opt. Soc. Amer. A 7, 1055-1073.

Ubeyli E.D., Guler I., 2005. *Adaptive neuro-fuzzy inference systems for analysis of internal carotid arterial Doppler signals*, Comp. Biol. Med., 35: 687–702.

Visee, H.F., Keunen, R.W., Pijlman, H.C., Vliegen, J.H., Tavy, D.L., Stam, K.J., Giller, C.A., 1995. *The physiological and clinical significance of nonlinear TCD waveform analysis in occlusive cerebrovascular disease*, Neurol. Res. 17:384–388.

Vliegen, J.H.R., Stam, C.J., Rombouts, S.A.R., Keunen R.W.M., 1996. *Rejection of the 'filtered noise' hypothesis to explain the variability of transcranial Doppler signals: a comparison of original TCD data with Gaussian-scaled phase randomized surrogate data sets*, Neurol. Res. 18: 19–24.

Webber, C.L. Jr., Zbilut, J.P., 1994. *Dynamical assessment of physiological systems and states using recurrence plot strategies*. Journal of Applied Physiology. 76:965-973.

Zbilut, J.P., Guiliani, A., Webber, C.L. Jr., 1998. *Recurrence quantification analysis and principle components in the detection of short complex signals*. Physics Letters A, 237:131-135.